Li *et al. Chin. J. Mech. Eng.* (2021) 34:15
https://doi.org/10.1186/s10033-021-00531-0

Chinese Journal of Mechanical Engineering

ORIGINAL ARTICLE Open Access

Unified Principal S–N Equation for Friction Stir Welding of 5083 and 6061 Aluminum Alloys

Xiangwei Li[1], Ji Fang[2*] and Xiaoli Guan[1]

Abstract

With the popularization of friction stir welding (FSW), 5083-H321 and 6061-T6 aluminum alloy materials are widely used during the FSW process. In this study, the fatigue life of friction stir welding with two materials, i.e., 5083-H321 and 6061-T6 aluminum alloy, are studied. Fatigue tests were carried out on the base metal of these two materials as well as on the butt joints and overlapping FSW samples. The principle of the equivalent structural stress method is used to analyze the FSW test data of these two materials. The fatigue resistances of these two materials were compared and a unified principal S–N curve equation was fitted. Two key parameters of the unified principal S–N curve obtained by fitting, C_d is 4222.5, and h is 0.2693. A new method for an FSW fatigue life assessment was developed in this study and can be used to calculate the fatigue life of different welding forms with a single S–N curve. Two main fatigue tests of bending and tension were used to verify the unified principal S–N curve equation. The results show that the fatigue life calculated by the unified mean 50% master S–N curve parameters are the closest to the fatigue test results. The reliability, practicability, and generality of the master S–N curve fitting parameters were verified using the test data. The unified principal S–N curve acquired in this study can not only be used in aluminum alloy materials but can also be applied to other materials.

Keywords: 5083 and 6061 aluminum alloy, Friction stir welding, Master S–N curve, Fatigue life

1 Introduction

Friction stir welding (FSW) technology has been widely adopted by the engineering community, and 5083-H32 and 6061-T6 aluminum alloys are widely used materials. Owing to the advantages of FSW technology, the FSW process is widely used for welding applications. Although a fatigue life analysis of the FSW technology used in the two materials mentioned above was conducted [1–4], most of the current studies have focused on the nominal stress fitted S–N curve of the FSW, resulting in different S–N curves for different materials and different welding joint forms. This is extremely inconvenient, and a large number of experiments are required to obtain the data.

Zhemchuzhikova et al. [5] discovered that the low dislocation density evolved in the stir zone hinders the initiation and growth of fatigue microcracks, and provides a superior FSW fatigue performance. Salari et al. [6] investigated the effect of the tool pin profile on FS-welded mechanical properties. The results indicate that the tool pin with a stepped conical threaded profile produced a weld with superior mechanical properties. Ilangovan et al. [7] joined two aluminum alloys AA6061 and AA5086 and examined the effect of the tool pin profile on the weld. Rodriguez et al. [8] examined the microstructure of the cross-sectional area of a dissimilar joint of 6061–7050 aluminum alloy and found that distinct lamellar bands and different degrees of mixing materials were associated with the tool rotational speed. The rupture occurred at the AA6061 side for all joints. Giraud et al. [9] presented the experimental results obtained through temperature and force measurements by varying the welding and rotational speeds during the FSW of dissimilar heat-treated aluminum alloys AA7020-T651 and AA6060-T6 by FSW. Another recent study by Pouget and Reynolds [10] also demonstrated that fatigue

*Correspondence: 66199315@qq.com
[2] College of Locomotive and Rolling Stock Engineering, Dalian Jiaotong University, Dalian 116028, China
Full list of author information is available at the end of the article

crack propagation in friction stir welded 2050 strongly depends on the presence of residual stress. However, they also indicated that other factors such as the microstructure and closure effects resulting from sources other than residual stress must be accounted for. Friction stir spot welding (FSSW) was conducted for dissimilar aluminum alloy (AA2024-T3 and AA5754-H114) sheets 2-mm thick at different tool rotational speeds, and the plunging times and process parameters were optimized using the Taguchi technique [11]. Friction stir lap welding joints were made for similar and dissimilar aluminum alloy (AA1100 to AA6061-T6) sheets 3-mm thick by varying the welding parameters, such as the tool rotation speeds. Many tests and inspections were also conducted, such as X-ray radiographic and tensile shear tests, to evaluate the weld quality and joint efficiency under different welding parameters [12]. In addition, the fatigue life of dissimilar friction stir spot welds in cross-tension and lap-shear specimens was predicted using the fatigue damage criteria [13]. The subsequent testing in Ref. [14] shows that the fatigue properties exceeded those reported for comparable AA6082-T6 gas metal arc butt welds and matched those reported for corresponding high-strength laser beams and friction stir weldments. The rotation and orbital speeds of tool are considered into variables, and the strength and mechanical properties, including the tensile strength, microhardness, mode I fracture energy, and mode I crack growth behavior of manufactured cylinders were investigated experimentally [15]. The mechanical properties, microstructure, and mode of failure in both types of FSSW were also evaluated and reported [16]. The reinforced welded joints of AA6061-T6 showed improvements in the unreinforced joint in terms of hardness and wear resistance owing to the high hardness and substantially increased grain refinement that occurred in the reinforced welded joints [17]. The tensile properties and high-cycle fatigue behavior of two tempers of AA7050 alloy (commercial T7451 and interrupted aging T6I4) were also investigated [18]. Thermomechanical fatigue tests under an in-phase temperature-mechanical strain combination was conducted in Ref. [19] on a type 316 LN austenitic stainless steel weld joint, and isothermal low-cycle fatigue tests were carried out at the maximum temperatures of the TMF cycling.

For the purpose of reliably predicting the fatigue life of FSW, the concept of structural stress and the mesh-insensitive main S–N curve method proposed in Refs. [20–23] were considered in the present study. The fatigue life prediction method of FSW was further studied using the principle of the main S–N curve method. The stress concentration factor (SCF) at the weld was calculated using the structural stress method. The test data and fatigue resistance of the FSW welding of these two materials were compared. The S–N curves of the 5083 and 6061 aluminum alloy base metal were acquired, and the unified main S–N curve equation was fitted for the butt and lap joints of the FSW. The principal of the unified main S–N curve formula for these two materials and the different welding forms were obtained. The unified main S–N curve equation was verified by two types of fatigue tests, bent and stretched. The rationality and applicability of the unified main S–N curve formula were also checked by analyzing the published test data. The test data are extremely useful for applying FSW, and a new method for an FSW fatigue life assessment was acquired.

2 Master S–N Curve Method

Structural stress is the main parameter of the master S–N curve equation and plays a key role in the fatigue life prediction of a welded structure. The structural stress value σ_s is equal to the sum of the membrane stress σ_m and bending stress, σ_b as shown in Figure 1.

According to the Paris formula, Dong [24] derived the master S–N curve equation using the stress intensity factor expression of structural stress:

$$\mathrm{d}a/\mathrm{d}N = C(M_{kn})^n(\Delta K_n)^m, \tag{1}$$

$$\Delta K = \sqrt{t}[\Delta\sigma_m f_m(a/t) + \Delta\sigma_b f_b(a/t)], \tag{2}$$

$$M_{kn} = \frac{M_{knT}f_m - r(M_{knT}f_m - M_{knB}f_b)}{f_m - r(f_m - f_b)}, \tag{3}$$

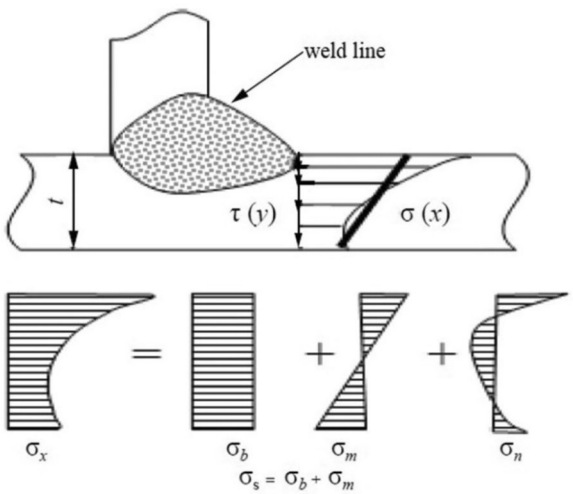

Figure 1 Structural stress and distribution at the weld toe

$$N = \int_{a_i/t\to 0}^{a/t=1} \frac{t\mathrm{d}(a/t)}{C(M_{kn})^n(\Delta K)^m} = \frac{1}{C}\cdot t^{1-\frac{m}{2}}\cdot(\Delta\sigma_s)^{-m}I(r), \quad (4)$$

The equivalent structural stress is written as follows:

$$\Delta S_s = \frac{\Delta\sigma_s}{t^{(2-m)/2m}\cdot I(r)^{1/m}}, \quad (5)$$

where t is the thickness of the plate, $I(r)$ is a dimensionless function of the bending ratio r, and $m = 3.6$.

According to the formula above, the master S–N curve equation can be defined as follows:

$$N = (\Delta S_s/C_d)^{1/h}. \quad (6)$$

3 FSW Fatigue Test

Fatigue and failure analyses were carried out on the butt and lap joints of friction stir welding in 5083-H321, 6061-T6 aluminum alloy materials. In addition, 5083-H321 is an Al-Mg type of rust proof aluminum alloy, and can achieve a medium strength and good corrosion resistance, and 6061-T6 aluminum alloy is an Al-Mg-Si wrought aluminum alloy material. After solution heat treatment and aging treatment, it can reach medium strength and high plasticity, and has a wide range of application [25, 26].

According to ISO 1099:2006 [27] Metallic materials-fatigue testing-axial force control method, to ensure that the sample breaks in the middle part, improve the test success rate. According to the test requirements, the sample materials of 5083-H321 and 6061-T6, butt, and lap joint samples were designed as shown in Figures 2, 3 and 4. The plate thickness is 6 mm, and the parameters of friction stir welding are shown in Table 1.

The process of the tensile fatigue test mainly refers to ISO 1099:2006. The main equipment and parameters of the fatigue test are shown in Table 2.

After the initial test period of approximately 200–300 cycles, when the load and displacement are substantially stable, the initial maximum ($+\delta_0$) and minimum ($-\delta_0$) displacement values were recorded (see Figure 5). The absolute values of the maximum and minimum displacements may differ depending on the response of the sample stiffness to different loads.

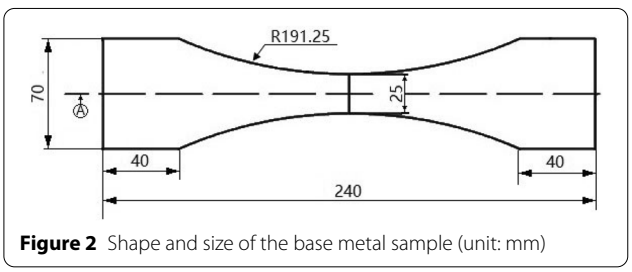

Figure 2 Shape and size of the base metal sample (unit: mm)

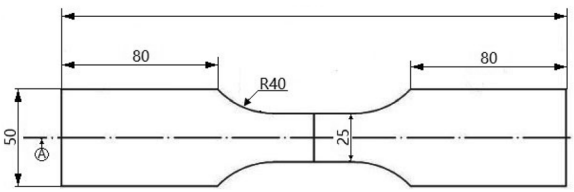

Figure 3 Shape and size of the butt specimen (unit: mm)

The fatigue test data of the 5083-H321 lap joint, butt joint, and metal base are shown in Figures 6, 7 and 8. The fatigue test data of the 6061-T6 lap joint, butt joint, and metal base are shown in Figures 9, 10 and 11. The horizontal coordinate is the sample ID, the Y-axis is the logarithm of the lifecycle, and the digital value at the top of the histogram is the measured nominal stress of each sample.

4 Data Statistics and Nominal Stress S–N Curve Fitting

The S–N curve was fitted according to the fatigue test data, and a statistical analysis was conducted using the least squares method provided in the S–N curve database software. The least squares method is a mathematical optimization technique [28]. The best function match of the data can be found by minimizing the sum of the square errors. The least squares method can be used to easily obtain unknown data and minimize the sum of the squares of the errors between the obtained and actual data. The algorithm for fitting the test data by the least squares is as follows.

The standard deviation is as follows:

$$\sigma = \sqrt{\frac{\sum_{i=1}^{n}(\log N_i - \bar{y}_i)^2}{n-1}}. \quad (7)$$

The standard S–N curve is as follows:

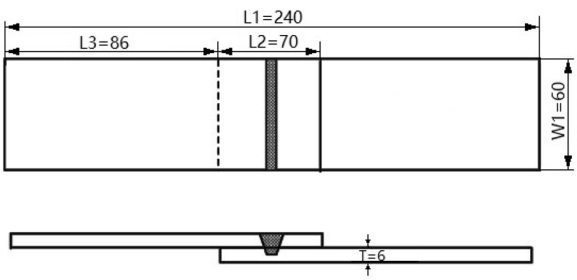

Figure 4 Shape and size of the lap test specimen (unit: mm)

Table 1 Parameters of friction stir welding

Materials	Joint type	Rotation speed (r/min)	Welding speed (m/min)	Misalig-nment	Assembly clearance
5083-H321	Butt	700	0.5	< 0.3	< 0.5
5083-H321	Lap	700	0.5	–	–
6061-T6	Butt	1500	0.6	< 0.3	< 0.5
6061-T6	Lap	1500	0.6	–	–

Table 2 Basic parameters of fatigue test

Type	Butt	Lap	Base metal
Stress ratio	− 1	− 1	− 1
Loading frequency (Hz)	15	15	118
Test equipment	Instron8802	Instron8802	Amsler 250 HFP 5100
Environment temperature (℃)	18–25	18–25	18–25
Nominal stress range (MPa)	98–154	20–70	45–180

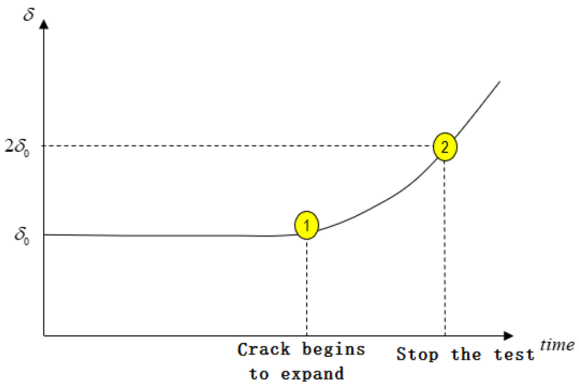

Figure 5 Absolute displacement versus stop time of test

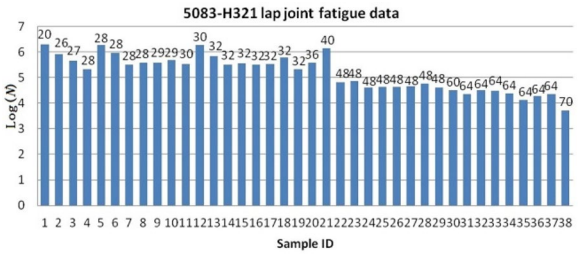

Figure 6 5083-H321 lap joint fatigue data

$$a = \lg C_d,\ b = -m, \tag{8}$$

$$\lg N = a \pm \mathrm{d}\sigma + b \cdot \lg \Delta S_s, \tag{9}$$

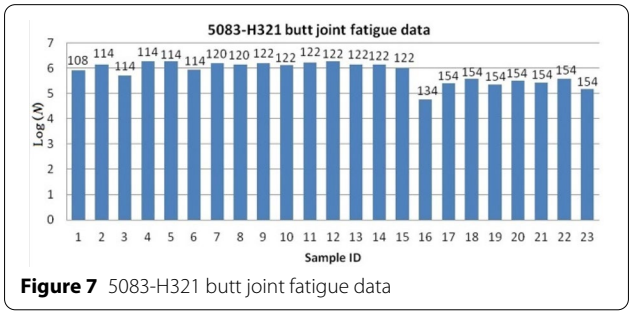

Figure 7 5083-H321 butt joint fatigue data

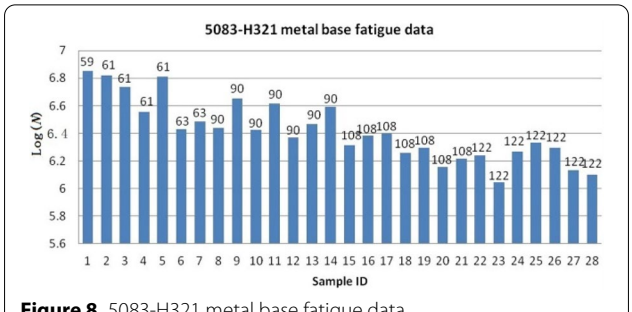

Figure 8 5083-H321 metal base fatigue data

$$N = \frac{10^{(\lg C_d \pm \mathrm{d}\cdot \lg \sigma)}}{\Delta S_s^m}. \tag{10}$$

Fatigue tests were carried out on the 5083-H321, 6061-T6 aluminum alloy base metal, and the butt and lap joints of friction stir welding. The fatigue tests on the base metal produced 70 effective results (28 specimens of 5083-H32 and 42 specimens of 6061-T6). The data obtained by the

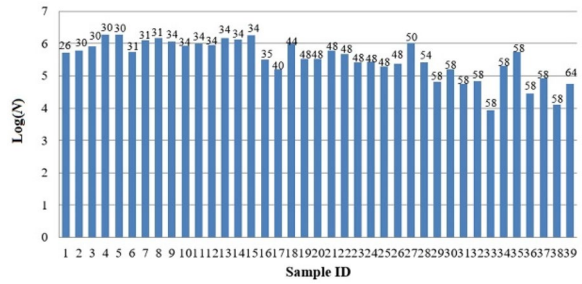

Figure 9 6061-T6 lap joint fatigue data

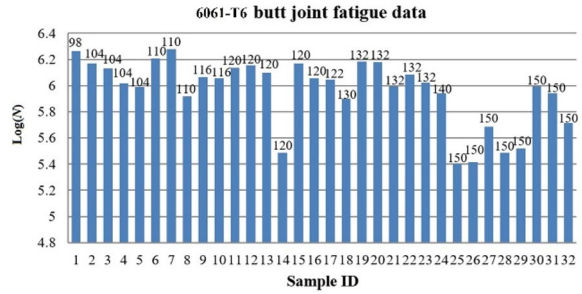

Figure 10 6061-T6 butt joint fatigue data

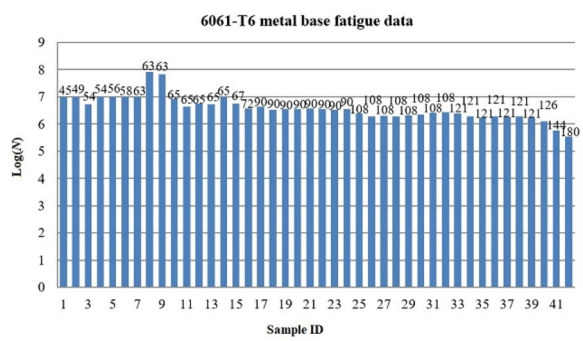

Figure 11 6061-T6 metal base fatigue data

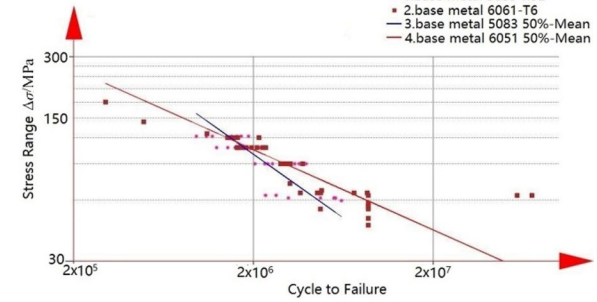

Figure 12 Fatigue test data of base metal (70 specimens in total)

Table 3 Nominal stress fitting curve parameters of base metal

Statistical basis	Base metal 5083		Base metal 6061	
	C_d	h	C_d	h
Mean	949807.0	0.6251	33768.7	0.3938
+ 2σ	1339127.8		52460.4	
− 2σ	673672.3		21736.8	
+ 3σ	1590066.7		65386.8	
− 3σ	567355.6		17439.6	

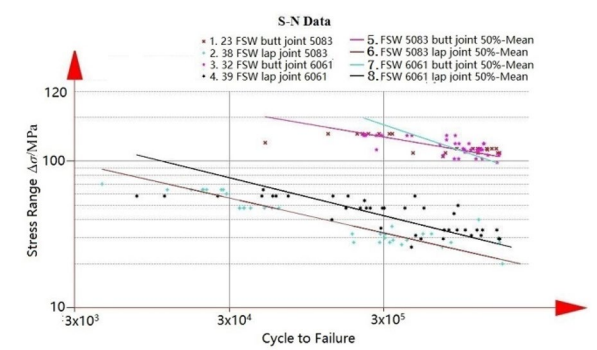

Figure 13 Weld fatigue test data (132 in total)

nominal stress variation range is shown in Figure 12, and the corresponding fitted S–N curve is shown in Table 3. A total of 132 effective test results were obtained in the fatigue test of the welding (28 lap joints of 5083-H321, 23 butt joints of 5083-H321, 39 lap joints of 6061-T6, and 32 butt joints of 6061-T6). The data obtained by the nominal stress variation range are shown in Figure 13. The corresponding fitted S–N curves are shown in Table 4.

The results of the nominal stress variation show that the base material of these two materials has the highest fatigue resistance, as shown in Table 5. The anti-fatigue capabilities of the 5083 and 6061 butt welding specimens are close to each other, and are slightly lower than that of the base metal. The fatigue life of the lap welding joint is the lowest, which is highly correlated with the local stress distribution at the welded line.

5 Master S–N Curve Fitting

The logarithm of the fatigue life number N belonging to the test specimen is the abscissa (X-axis). The logarithm of the equivalent structural stress variation range ΔS is the ordinate (Y-axis). The curve shows the relationship

Table 4 FSW nominal stress fitting curve parameters

Statistical basis		Mean	+ 2σ	− 2σ	+ 3σ	− 3σ
Butt 5083	C_d	1436.4	1809.6	1140.2	2031.1	1015.8
	h	0.1791				
Lap5083	C_d	676.0	911.5	501.3	1058.5	431.7
	h	0.2383				
Butt 6061	C_d	16195.4	22134.7	11849.8	25877.0	10136.1
	h	0.3542				
Lap 6061	C_d	1159.4	1835.6	732.3	2309.6	582.0
	h	0.2594				

Table 5 Master S–N fitting curve parameters of the base metal

Statistical basis	Parameter	
	C_d	h
Mean	64497.1	0.4353
+ 2σ	99386.0	
− 2σ	41855.8	
+ 3σ	123372.2	
− 3σ	33718.1	

between the stress intensity and fatigue life of a specimen under certain cycle characteristics and is called the equivalent structural stress-life curve, or the master S–N curve [29].

The master S–N curve fitted data used 5083-H321, 6061-T6 aluminum-alloy based metal, and a fatigue test of the butt and lap friction stir welding specimens. Among them, 70 effective results were obtained in the fatigue test of the base metal (28 in 5083 and 42 in 6061). A total of 132 effective test results were obtained in the fatigue test of the welding joints (28 lap joints of 5083, 23 butt joints of 5083, 39 lap joints of 6061, and 42 butt joints of 6061). According to the master S–N curve method and the mathematical statistical analysis method, the effective test data were analyzed, and the master S–N curve shown in Figures 14 and 15 were obtained. The parameters of the correlation curve are shown in Tables 5 and 6.

The master S–N curve fitting data above shows that the master S–N curves of the 5083-H321 and 6061-T6 aluminum alloy base metal with equivalent structural stress statistics were distributed within the same interval with a standard deviation of 0.2157 and a small dispersion. The master S–N curves of the 5083-H321 and 6061-T6 materials for the butt joint and lap friction stir welded specimens were also distributed within the same interval, the standard deviation was 0.4615, and the dispersion

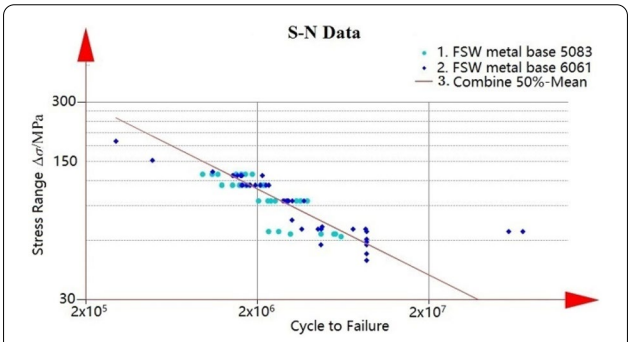

Figure 14 Master S–N fatigue test data of base metal (70 specimens in total)

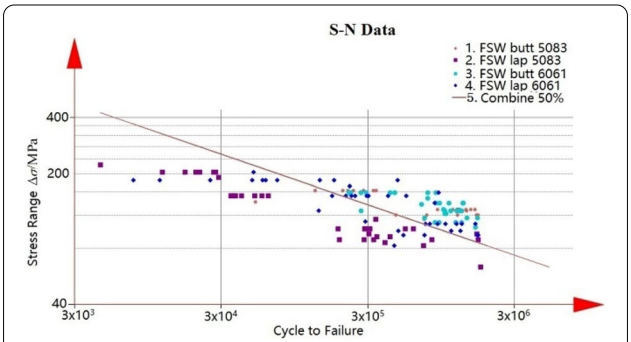

Figure 15 Master S–N fatigue test data of weld joint

Table 6 Master S–N fitting curve parameters of FSW

Statistical basis	Parameter	
	C_d	h
Mean	4222.5	0.2693
+ 2σ	7483.1	
− 2σ	2382.7	
+ 3σ	9961.8	
− 3σ	1789.8	

was not high. Therefore, the parameters of the master S–N curve above can be used to calculate the fatigue life. In addition, the data analysis shows that the difference between the master S–N curve data obtained by the equivalent structural stress is not obvious, and the difference between the 5083-H321 and 6061-T6 materials is not obvious. Thus, the high-strength aluminum alloy 6061-T6 does not exhibit a better fatigue performance than the 5083-H321 alloy. This indicates that the increase in the static load strength of the aluminum alloy does not significantly improve the fatigue strength of FSW joints. This conclusion is similar to the fatigue performance of fusion welding.

6 Master S–N Curve Comparison Analysis

To further analyze the fatigue performance of FSW, the FSW data were compared with the master S–N curve of the welding of the steel and aluminum alloy materials provided in the ASME standard (see Figure 16). The comparison results show that the FSW mean S–N curve is between the melted S–N curve and the mean 50% master S–N curve, which proves that the fatigue resistance of the FSW of an aluminum alloy material is significantly higher than that of a fusion-welded aluminum alloy material. This has a strong correlation with the properties of the welded tissue, stress concentration, and factors such as welding defects and distribution of residual stress.

A comparison of the master S–N curve of FSW, fusion welded steel, and aluminum are shown in Figure 14. At the same time, the fatigue performance of FSW and the fatigue properties of the base metal were compared (see Figure 17). The nominal stress method and equivalent structural stress method were applied for a comparative analysis. The results show that when the nominal stress method is used for a statistical analysis, the fatigue properties of the base metal are close to the fatigue life of the

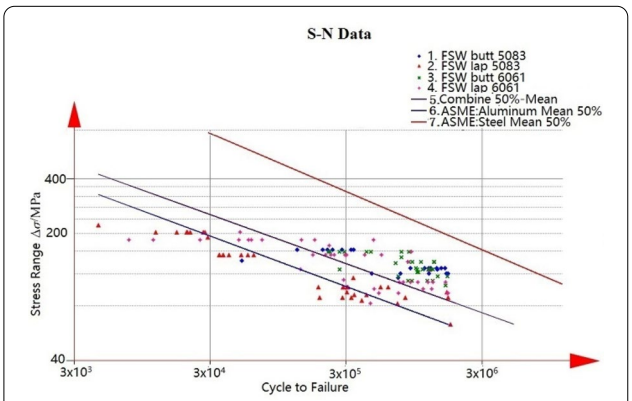

Figure 16 Comparison of the master S–N curves of FSW, welded steel, and aluminum

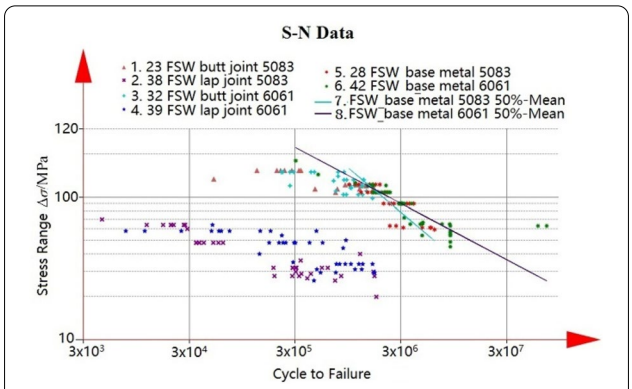

Figure 17 Fatigue life comparison between FSW and normal welding using nominal stress

butt FSW, but significantly higher than the fatigue life of the lap joint. However, when the fatigue life of FSW with the equivalent structural stress was compared with the fatigue life data of the base metal (Figure 18), the distribution interval was not obvious, and the fatigue life of the base metal was only slightly better than the fatigue life of the FSW. This further indicates that the FSW fatigue life is close to the fatigue life of the base metal when the fatigue life analysis is conducted using the equivalent structural stress method. It also proves the advantages and potential engineering application of an FSW welded structure.

7 Master S–N Curve Example Verification

To verify the FSW nominal stress fitting curve parameters of Table 4 and the FSW master S–N fitting curve parameters listed in Table 6, the lap bending test and the butt tensile test were compared using the 6005 aluminum alloy. First, the bending fatigue test was carried out on a lap weld using a 6005 aluminum alloy. Two tests were carried out, the load was 4–0.4 kN and 4.25–0.425 kN, respectively. To ensure the test accuracy, the loading

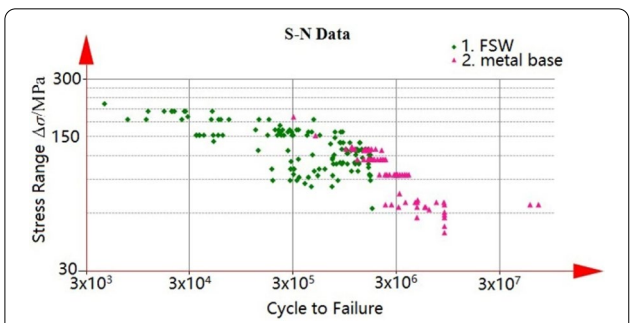

Figure 18 Fatigue life comparison between FSW and base metal using equivalent structural stress

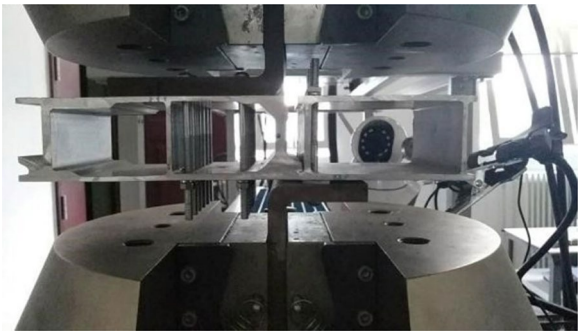

Figure 19 Bending fatigue test of 6005 aluminum alloy FSW joint

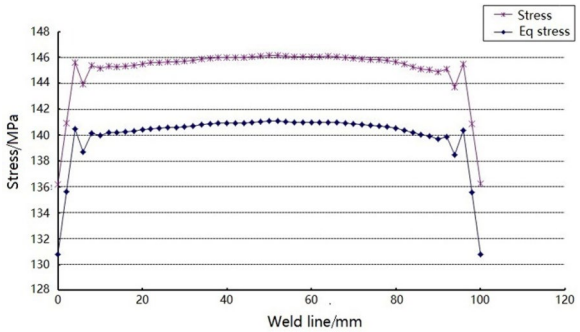

Figure 20 Calculated stress of lap joint structure of 6005 aluminum alloy

frequency was set to 1 Hz. The test specimen and test load are shown in Figure 19.

The nominal stress of the section at the joint was calculated according to the material mechanics formula. The maximum principal stress, structural stress, and equivalent structural stress calculated by the structural stress method are shown in Figure 20, Table 7, and Table 8.

The tensile fatigue test was then carried out on the butt weld of the 6005 aluminum alloy. Two tests were conducted. The loads of both groups were 0.3–30 kN, the loading frequency was set to 10 Hz, and the test specimen and test equipment were as shown in Figure 21.

The nominal stress of the section at the joint can be calculated using Eq. (11). The maximum principal stress distribution is acquired through a static analysis using ANSYS software, as shown in Figure 22. The maximum principal stress, structural stress, and equivalent structural stress calculated based on the SSM are shown in Figure 23 and Table 9.

$$\sigma_m(mean) = \frac{F}{A} = \frac{F}{b \cdot t} = \frac{30000}{5 \times 60} = 100 \text{ MPa}. \quad (11)$$

Through a comparison of the above statistical data, in the two types of fatigue tests of the bending and stretching, the life results calculated using the equivalent structural stress range and the mean 50% master S–N curve parameters are closest to those of the fatigue test. For example, in the bending test, the calculation results of

Table 7 Comparison of fatigue test results and evaluation life of test sample type 1

Stress type	Stress value (MPa)	50% S–N curve fatigue assessment life (times)	Load range (kN)	Test fatigue life (times)
$\Delta\sigma$(Nominal stress range)	156.8	485317	4.0–0.4	446048
$\Delta\sigma_{max}$(Finite element maximum principal stress range)	103.5	1564338		
$\Delta\sigma_s$(Structural stress range)	146.2	211510		
ΔS(Equivalent structural stress range)	141.1	302715		

Table 8 Comparison of bending fatigue test results and evaluation life of test sample type 2

Stress type	Stress value (MPa)	50% S–N curve fatigue assessment life (times)	Load range (kN)	Test fatigue life (times)
$\Delta\sigma$(Nominal stress range)	166.6	409118	4.25–0.425	194606
$\Delta\sigma_{max}$(Finite element maximum principal stress range)	110.1	1317403		
$\Delta\sigma_s$(Structural stress range)	155.3	177495		
ΔS(Equivalent structural stress range)	149.9	241807		

Figure 21 Fatigue test of butt weld

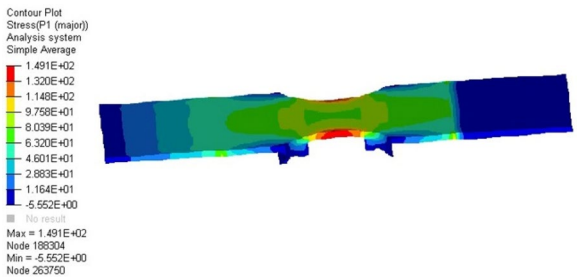

Figure 22 FEA calculation of 6005 aluminum alloy butt weld test sample

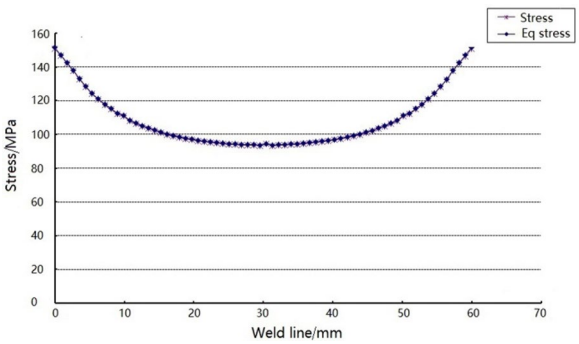

Figure 23 Calculated structural stress of butt weld sample with 6005 aluminum alloy

the test sample type 1 were 30.27 million times, and the corresponding fatigue test result was 44.60 million times. The calculation result of test sample type 2 was 24.18 million times, and the fatigue test result was 19.46 million times. For the tensile test, the calculation result was 24.46 million times, and the fatigue test results of test sample type 2 were 39.44 million and 23.94 million times, respectively. However, when the nominal stress method was used, and the stress gradient did not change significantly, and the selected S–N curve data corresponded to the test, the effect was acceptable. For example, the first type of bending test can obtain good results, but when the stress gradient. When the value is larger, the error between the calculated result and the test is larger, as indicated by the results of the tensile test in Table 9. At present, the results of the calculation of the maximum principal stress range obtained through a finite element calculation are unreliable, and are related to the size of the finite element unit and the change in the stress gradient. It can be seen through a comparison with the experimental data that the mean 50% master S–N curve fitting parameters are reliable, and results closer to those of the test can be obtained. Therefore, according to the FSW master S–N fitting curve parameters in Table 6, the FSW welds of the series 5 and 6 aluminum alloys can be evaluated using the equivalent structural stress method. In addition, considering the reliability and safety of the structural design, when using FSW technology for the structural design, it is recommended to use FSW master S–N fitting curve parameters of -2σ shown in Table 6 for a fatigue life calculation.

8 Master S–N Curve Applicability Verification

To further verify the applicability of the FSW master S–N fitting curve parameters in Table 7, the related literature information was researched, and the FSW test data in the literature were entered into the database. The equivalent structural stress method was used for comparison with the relevant fatigue test data, including related test data from Zhejiang University of Technology (31 samples), Shandong University (47 samples), Kunming University of Science and Technology (9 samples), and Tongji University (14 samples) [30–33]. The test data included butt, lap joint FSW welds, and three aluminum alloy materials 6082-T6, 6005A, and 2024-T351. The above data were compared with the test data in this study, as shown in Figure 24.

It can be seen from Figure 24 that only the experimental data of Kunming University of Science and Technology have a certain error in comparison with the other test data, which may be related to the presence of coupler-shaped defects in the specimens described in the literature. The defect has a sharp notch shape with a serious stress concentration, which is equivalent to a pre-existing crack; however, whether it is related to other factors remains to be determined through further studies.

The other test data are basically within the same distribution area as the test data in this report. The test data from Shandong University are slightly better. Therefore, it can be shown that the master S–N curve data provided

Table 9 Comparison of fatigue test results and evaluation of life of butt test specimens

Stress type	Stress value (MPa)	50% S–N curve fatigue assessment life (times)	Load range (kN)	Test fatigue life (times)
ΔS(Nominal stress range)	99.0	1778354	0.3–30	type1: 349440 type2: 239440
$\Delta\sigma_{max}$(Finite element maximum principal stress variation range)	147.6	575864		
$\Delta\sigma_s$(Structural stress range)	149.5	198236		
$\Delta\sigma_s$(Equivalent structural stress variation range)	150.1	240612		

in this report can also be applied to the FSW weld evaluation of these two materials, 6082-T6 and 6005A. This further proves the applicability and advantages of the equivalent structural stress method for fatigue life assessment.

9 Conclusions

(1) Fatigue tests were carried out on specimens of 5083-H321, 6061-T6 aluminum alloy, butt joints, and lap friction stir welding. The results from the range of nominal stress variation show that the anti-fatigue capability of the base metal is the highest, and the anti-fatigue capabilities of the 5083 and 6061 butt welding samples are close to each other, and are slightly lower than that of the base metal. The 5083 and 6061 lap welds have the lowest fatigue resistance, which is strongly correlated with the local stress distribution at the weld.

(2) The equivalent principal stress method was used to fit the unified master S–N curve of the two materials according to the friction stir welding fatigue test data of the 504-1H321 and 6061-T6 aluminum alloy, and butt and lap joints. The mean 50% S–N curve parameter C_d is 4222.5, h is 0.2693, and the data fit well. The mean master S–N curve of FSW is between that of the fusion welding steel and the aluminum mean 50% master S–N curve, which proves that the fatigue resistance of the aluminum alloy material is significantly higher than that of the melted aluminum alloy material during FSW.

(3) The master S–N curve parameters were verified based on bending and tensile fatigue specimens. The life results calculated through the equivalent structural stress range, and the mean 50% master S–N curve parameters are closer to the fatigue test results. Therefore, the unified master S–N fitted curve parameters of FSW, according to five series and six series aluminum alloys, can be evaluated using the equivalent structural stress method according to the main S–N curve.

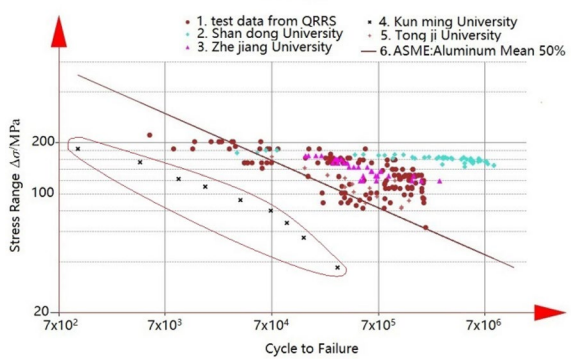

Figure 24 Comparison of applicability of the master S–N fit curve

Acknowledgements
The authors sincerely thank Professor Wenzhong Zhao of Dalian Jiaotong University for his critical discussion and reading during manuscript preparation.

Authors' contributions
XL is in charge of the whole trial; JF assisted with sampling and wrote the manuscript; and XG assisted with laboratory analyses. All authors read and approved the final manuscript.

Authors' Information
Xiangwei Li, born in 1968, professor-level senior engineers, doctors, and CRRC scientists, mainly engaged in research on vehicle vibration fatigue test technology.

Ji Fang, born in 1981, associate professor, doctor, mainly engaged in vehicle dynamics and vibration fatigue research.

Xiaoli Guan, born in 1973, senior engineer, CRRC QIQIHAR ROLLING STOCK CO., LTD, mainly research direction is railway product finite element analysis.

Funding
Supported by Department of Education of Liaoning Province (Grant No. JDL2020019), and Dalian High Level Talents Project (Grant No. 2017RQ132).

Competing interests
The authors declare no competing financial interests.

Author Details
[1] CRRC QIQIHAR ROLLING STOCK CO.,LTD, Qiqihar 161000, China. [2] College of Locomotive and Rolling Stock Engineering, Dalian Jiaotong University, Dalian 116028, China.

Received: 3 January 2020 Revised: 6 December 2020 Accepted: 4 January 2021
Published online: 22 January 2021

References

[1] Ahmed B Mousa, Mousa Ahmed B, Abbass Muna K, et al. Fatigue behavior and fractography in friction stir welding zones of dissimilar aluminum alloys (AA5086-H32 with AA6061-T6). *Materials Science and Engineering*, 2020, 881(1): 1-15.

[2] A Chen, J Yang, X M Chen, et al. Fatigue property of friction stir welded butt joints for 6156-T6 aluminum alloy. *Materials Science Forum*, 2019, 960(1): 45-50.

[3] X Zhang, L X Wei, Y B Wang. Processing technology of aluminum alloy side wall of railway freight car. *Metal Processing*, 2016(31): 124-127.

[4] P M Kumar, K Balamurugan, S Gowthaman, et al. Fractography analysis and modeling studies on friction stir welded AA6061/SiC composite. *Journal of Advanced Microscopy Research*, 2018, 13(1): 72-78.

[5] Daria Zhemchuzhikova, Sergey Mironov, Rustam Kaibyshev. Fatigue performance of friction stir welded Al-Mg-Sc alloy. *Metallurgical and Materials Transactions*, 2019, 48(1): 150-158.

[6] E Salari, M Jahazi, A Khodabandeh, et al. Influence of tool geometry and rotational speed on mechanical properties and defect formation in friction stir lap welded 5456 aluminum alloy sheets. *Mater and Design*, 2014, 58(1): 381-389.

[7] M Ilangovan, S R Boopathy, Balasubramanian. Effect of tool pin profile on microstructure and tensile properties of friction stir welded dissimilar AA6061-AA5086 aluminium alloy joints. *Defence Technology*, 2015, 11(2): 174-184.

[8] R I Rodriguez, J B Jordon, P G Allison, et al. Microstructure and mechanical properties of dissimilar friction stir welding of 6061-to-7050 aluminum alloys. *Mater and Design*, 2015, 83(1): 60-65.

[9] L Giraud, H Robe, C Claudin, et al. Investigation into the dissimilar friction stir welding of AA7020-T651 and AA6060-T6. *Journal of Materials Processing Technology*, 2016, 235(1): 220-230.

[10] G Pouget, A P Reynolds. Residual stress and microstructure effects on fatigue crack growth in AA2050 friction stir welds. *International Journal of Fatigue*, 2008, 30(1): 463-472.

[11] Muna K Abbass, Sabah Kh Hussein, Ahmed A Khudair. Optimization of mechanical properties of friction stir spot welded joints for dissimilar aluminium alloys (AA2024-T3 and AA5754- H114). *Arabian Journal for Science and Engineering*, 2016, 41(11): 4563-4572.

[12] Muna K Abbass, Kareem M Raheef. Evaluation of the mechanical properties of friction stir. lap welded joints for dissimilar aluminum alloys(AA1100 To AA6061). *2018 1st International Scientific Conference of Engineering Sciences - 3rd Scientific Conference of Engineering Science (ISCES)*, IEEE, 2018: 192-197.

[13] Aghabeigi, Mahya, Hassanifard, et al. Evaluation of different strain-based damage criteria for predicting the fatigue life of friction stir spot-welded joints under multi-axial loading conditions. *Journal of Materials Design and Application*, 2020, 234(1):156-166.

[14] L Sandnes, Y Grong, T Welo, et al. Fatigue properties of AA6060-T6 butt welds made by hybrid metal extrusion & bonding. *Fatigue & Fracture of Engineering Materials & Structures*, 2020, 43(1): 1-9.

[15] M R M Aliha, Seyed Mohammad, Navid Ghoreishi, et al. Mechanical and fracture properties of aluminium cylinders manufactured by orbital friction stir welding. *Fatigue & Fracture of Engineering Materials & Structures*, 2020, 43(1): 9-12.

[16] S Suresh, K Venkatesan, E Natarajan, et al. Evaluating weld properties of conventional and swept friction stir spot welded 6061-T6 aluminium alloy. *Materials Express*, 2019, 9(8): 851-860.

[17] E T Abioye, H Zuhailawati, S A Anasyida, et al. Investigation of the microstructure mechanical and wear properties of AA6061-T6 friction stir weldments with different particulate reinforcements addition - ScienceDirect. *Journal of Materials Research and Technology*, 2019, 8(5): 3917-3928.

[18] AMBS Antunes, CARP Baptista, MJR Barboza , et al. Effect of the interrupted aging heat treatment T6I4 on the tensile properties and fatigue resistance of AA7050 alloy. *Journal of the Brazilian Society of Mechanical Sciences and Engineering*, 2019, 41(8): 1-8.

[19] T S Kumar, A Nagesha, R Kannan. Thermal cycling effects on the creep-fatigue interaction in type 316LN austenitic stainless steel weld joint. *International Journal of Pressure Vessels and Piping*, 2019, 178: 104-109.

[20] Niu Kun. *Microstructure and properties of friction stir welded joints of aluminum alloy and magnesium alloy heterogeneous materials*. Changchun: Jilin University, 2012.

[21] R Pan. *Effect of material properties on weld formation and mechanical properties of friction stir welding of aluminum alloy*. Nanchang: Nanchang Aeronautical University, 2015.

[22] H Y Wang, W J Qi, D Nong. Microstructure and properties of friction stir weldindg 6061 aluminium alloy joint. *Chinese Journal of Rare Metals*, 2015, 35(5): 638-642.

[23] P Dong, J K Hong, D A Osage, et al. Master S-N curve method for fatigue evaluation of welded components. *Welding Research Council Bulletin*, 2002(474): 1-44.

[24] P Dong. Length scale of secondary stresses in fracture and fatigue. *International Journal of Pressure Vessels and Piping*, 2007, 85(3): 128-143.

[25] Z J Lv, H Zhang, Y Guo. Processes and properties of friction stir welding joint of 6061 Al-alloy with zero title angle. *Journal of Netshape Forming Engineering*, 2018, 10(4): 108-113.

[26] H S Qin, X Q Yang. Performances of fatigue crack growth for aluminum friction stir welds and base materials. *Journal of Aeronautical Materials*, 2017, 37(5): 41-47.

[27] The International Organization for Standardization. *Metallic materials fatigue testing axial force control method*. Switzerland: Technical Committee ISO/TC, 2006.

[28] ASME. VIII DIV 2-2007 ASME boiler and pressure vessel code. New York: The American Society of Mechanical Engineers, 2007.

[29] W Z Zhao, H L Wei, J Fang. The theory and application of the virtual fatigue test of welded structures based on the master S-N curve method. *Transactions of the China Welding Institution*, 2014, 35(5): 75-78.

[30] Peng Mi, Ruijie Wang, Qinghe Yang. Study on kissing bond depth on the fatigue strength of AA5083 FSW butt joints. *Mechanical Science Technology for Acrospace Engineering*, 2020, 4: 1-7.

[31] Baohai Zhang. *Study on the microstructure and mechanical properties of bobbin tool friction stir welding of 6082-T6 aluminum alloy*. Jinan: Shandong University, 2017. (in Chinese)

[32] Rongkang Chen, Chunfang Sun, Ying Dai. Fatigue property of friction stir welded extruded aluminium alloy 6005A. *Chinese Quarterly Mechanics*, 2012. (in Chinese)

[33] Qingfeng Wang. *Friction stir welding of 6005A-T6 aluminum alloy for the metro vehicles car body*. Hangzhou: Zhejiang University of Technology, 2015. (in Chinese)